



Full paper/Mémoire

DFT, FT-Raman, FT-IR, solution and solid state NMR studies of 2,4-dimethoxyphenylboronic acid

Özgür Alver^{a,b,*}^a Plant, Drug and Scientific Research Centre, Anadolu University, Eskişehir, Turkey^b Department of Physics, Science Faculty, Anadolu University, Eskişehir, Turkey

ARTICLE INFO

Article history:

Received 7 April 2010

Accepted after revision 4 November 2010

Available online 26 January 2011

Keywords:

2,4-Dimethoxyphenylboronic acid

IR and Raman spectra

Vibrational wavenumbers

DFT

(CP/MAS) NMR

ABSTRACT

The possible stable forms and molecular structures of 2,4-dimethoxyphenylboronic acid (2,4-dmpba) have been experimentally and theoretically studied using FT-IR, Raman and solution and solid state NMR spectroscopic methods. FT-IR and Raman spectra were recorded in the region of 4000–400 cm⁻¹. ¹³C cross-polarization magic-angle spinning NMR and solution phase ¹H, ¹³C and HETCOR NMR spectra of 2,4-dmpba ((CH₃O)₂C₆H₃-B(OH)₂) have been reported. The optimized geometric structures concerning to the minimum on the potential energy surface was investigated by Becke-3-Lee-Yang-Parr (B3LYP) hybrid density functional theory method together with 6-31++G(d,p) basis set. The vibrational wavenumbers and ¹H, ¹³C NMR chemical shifts of 2,4-dmpba have been calculated by means of B3LYP density functional methods with 6-31++G(d,p) basis set. Reliable vibrational assignments were made on the basis of total energy distribution (TED) calculated with scaled quantum mechanical (SQM) method. Comparison between the experimental and the theoretical results indicates that density functional B3LYP method is able to provide satisfactory results for predicting vibrational wavenumbers and nuclear magnetic shielding tensors. Furthermore, the cis-trans (ct) form of 2,4-dmpba with Cs point group has been found to be the most stable conformer.

© 2010 Académie des sciences. Published by Elsevier Masson SAS. All rights reserved.

1. Introduction

Boron and boronic acid containing organic compounds have become an object of recent increasing interest due to their extensive application potentials in the field of material science, supramolecular chemistry, analytical chemistry, medicine, biology, catalysis, organic synthesis and crystal engineering. A wide range of biologically important boronic acid derivatives have been synthesized as anti-metabolites [1–8]. Boron-based compounds show preferential localization in tumor containing tissues making the boron-10 neutron capture therapy possible [9]. The boronic acid moiety has been also employed in the synthesis of anti-tumor and anti-viral agents [10].

Density functional theory (DFT) calculations provide excellent agreement with experimental vibrational frequencies of organic compounds, if the calculated frequencies are scaled to compensate for the approximate treatment of electron correlation, basis set deficiencies and anharmonicity [11–17]. Moreover, the Gauge Including Atomic Orbitals/Density Functional Theory (GIAO/DFT) approach is extensively used for the calculations of chemical shifts of different types of compounds [18–23].

Solid and solution state NMR methods are very useful tools for structural identification of isolated or synthesized molecules and they allow to get faster and easier structural information. The standard 1D and 2D hetero- and homonuclear NMR experiments are greatly helpful for assignment of organic compounds and effective to afford molecular structure information [24–26]. Biological activity is closely related to the molecular preferences [18]; therefore, especially solid state NMR and theoretical data

* Corresponding author.

E-mail address: ozgur.alver@anadolu.edu.tr.

of 2,4-dmpba seem to be valuable. Since shielding is very sensitive to the geometric structure and chemical environment, DFT calculations can be used to investigate solid state structure and inter–intramolecular interactions [27,28]. In this work, the most stable conformers of 2,4-dmpba have been studied within the framework of DFT. A detailed interpretation of the vibrational spectra of 2,6-dmpba has been conducted on the basis of the calculated total energy distribution (TED) [29]. ^1H , ^{13}C (CP/MAS) NMR chemical shifts and HETCOR spectra of 2,4-dmpba have been reported. The vibrational wavenumbers, ^1H , ^{13}C chemical shifts and some important structural parameters have been also calculated at B3LYP level of theory using 6-31++G(d,p) basis set. The results of the theoretical and spectroscopic studies are reported here.

2. Experimental

A commercial sample of 2,4-dmpba was purchased and used without further purification. FT-IR spectrum of 2,4-dmpba was recorded using Perkin Elmer Spectrum 2000 spectrometer with the resolution of 2 cm^{-1} in the spectral region of $4000\text{--}400\text{ cm}^{-1}$. The Raman spectrum was obtained using a Bruker Senterra Dispersive Raman microscope spectrometer with 532 nm excitation from a 3B diode laser having 3 cm^{-1} resolution in the spectral region of $3700\text{--}400\text{ cm}^{-1}$. All NMR spectra of the compounds were recorded on a Bruker Avance II 500 NMR spectrometer at ambient probe temperature. The operating frequencies were 500.13 and 125.76 MHz ^1H and ^{13}C , respectively. ^1H and ^{13}C NMR spectra were measured in CDCl_3 , with tetramethylsilane (TMS) as internal reference in 5 mm NMR tubes. The pulse conditions used in the solution state NMR experiments were as following: for 2,4-dmpba, ^1H NMR spectra: spectrometer frequency (SF) 500.13 MHz, spectral width (SW) 5498.53, acquisition time (AQ) 5.96 s, number of scan (NS) 32, P1 14.15 μs , receiver gain (RG) 50.8, digital resolution (DR) 23 Hz, dwell time (DW) 90.93 μs , prescan delay (DE) 6.00 μs ; ^{13}C NMR spectra: SF 125.76 MHz, SW 29761.90, AQ 1.10 s, NS 64, P1 8.30 μs , RG 724, DR 21 Hz, DW 16.80 μs , DE 6.00 μs . The (CP/MAS) NMR experiments were carried out on a Bruker Avance-300 WB equipped with a 4 mm (CP/MAS) probe. The operating frequencies were 75.47 and 30.41 MHz for ^{13}C . External referencing was performed relative to glycine molecule. All solid experiments were performed using high power hydrogen decoupling. A zirconium oxide rotor with a 4 mm diameter was used to acquire the NMR spectra of ^{13}C and sample was spun at 7 kHz. For ^{13}C (CP/MAS) NMR spectroscopy of 2,4-dmpba, contact time of 2.0 ms, repetition time of 5.0 s and spectral width of 24038.46 Hz and 6.0 μs delay time before acquisition were used for accumulation of 512 scans.

3. Calculations

Many possible conformers could be proposed for 2,4-dmpba but here the discussion is limited to $\text{tt}(\text{C}_1)$, $\text{ct}(\text{C}_1)$, $\text{cc}(\text{C}_1)$, $\text{tt}(\text{Cs})$, $\text{ct}(\text{Cs})$ and $\text{cc}(\text{Cs})$ isomers (Fig. 1), where t and c stand for trans and cis, respectively. For the calculations, six forms of 2,4-dmpba were first optimized by B3LYP with

6-31++G(d,p) basis set in the gas phase. The optimized geometric structures relative to the minimum on the potential energy surface were provided by solving the self-consistent field (SCF) equation iteratively. For the vibrational calculations, the vibrational wavenumbers of 2,4-dmpba were calculated using the same method and the basis set under the keyword `freq=Raman`. The assignments of the vibrational modes of the title molecule were provided by animation option of the GaussView package program for the B3LYP/6-31++G(d,p) level of calculation. TED calculations, which show the relative contributions of the redundant internal coordinates to each normal vibrational mode of the molecule and thus make it possible to describe the character of each mode numerically, were carried out by the scaled quantum mechanical (SQM) program [17,29] using the output files created at the end of the wavenumber calculations. For the NMR calculations, all suggested forms of the title molecule were first fully optimized at 6-31++G(d,p) level in chloroform using the PCM method [30]. After optimization, ^1H and ^{13}C NMR chemical shifts (δ_{H} and δ_{C}) of 2,4-dmpba were calculated using the GIAO method [31] in chloroform at the B3LYP/6-31++G(d,p) level. Relative chemical shifts were then estimated using the corresponding TMS shieldings calculated in advance at the same theoretical levels as the references. All calculations were performed using Gaussian 03 program on a personal computer [32].

4. Results and discussion

4.1. Geometrical structures

The optimized geometric parameters (bond lengths, bond and dihedral angles) calculated with B3LYP/6-31++G(d,p) are listed in Table 1. Considering the calculated geometric parameters, it is possible to construct the structures of six possible isomers given in Fig. 1. The phenylboronic acid molecule was studied by X-ray diffraction [33]. Since the crystal structure of 2,4-dmpba is not available in the literature up to now, the structural parameters were compared with phenylboronic acid. The magnitude of $\text{D}(3;9;10;11)$ and $\text{D}(3;9;12;13)$ angles are about 0.00° and 180.00° for $\text{ct}(\text{Cs})$ and $\text{ct}(\text{C}_1)$ conformers, which indicates that both hydrogens are almost in the O–B–O plane. In general, B–O distances are 1.359 \AA [34] in compliance with strong p–interactions. Chen et al. [10] found nearly the same value for this bond length using HF/6-31G(d) levels of theory for the few boronic acids including phenylboronic acid. For the 2,4-dmpba molecule B–O distances including $\text{ct}(\text{Cs})$ and $\text{ct}(\text{C}_1)$ forms were found from 1.371 to 1.375 \AA . Bhat et al. [35] calculated B–C bond length 1.566 \AA and 1.567 \AA for form of phenylboronic acid using B3LYP and MP2 methods, respectively. The B–C bond length for the title molecule is calculated as 1.567 \AA for $\text{ct}(\text{Cs})$ and $\text{ct}(\text{C}_1)$ forms. The calculated B–O and B–C bond lengths for 2,4-dmpba are in good agreement with previously reported data found in the X-ray structure [36]. Regarding the relative energy differences given in Table 2, the relative mole fractions of $\text{tt}(\text{C}_1)$, $\text{cc}(\text{C}_1)$, $\text{tt}(\text{Cs})$ and $\text{cc}(\text{Cs})$ could be ignored since their relative energy

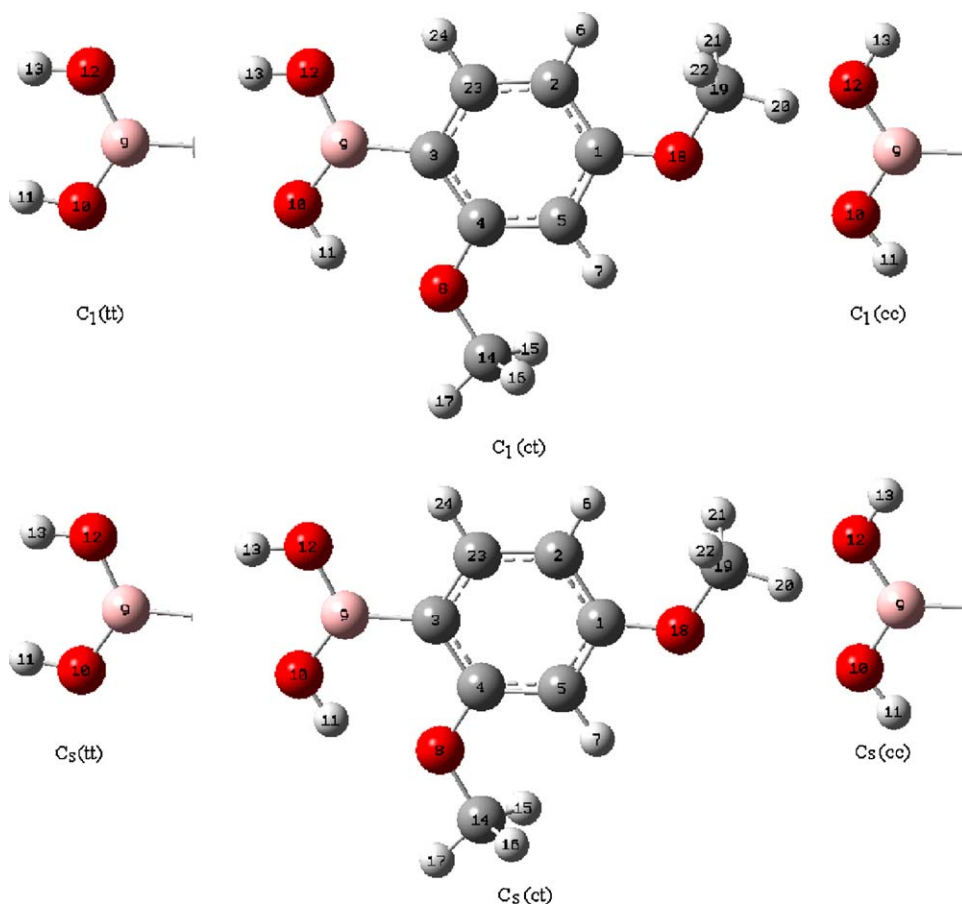


Fig. 1. The theoretical optimized possible six geometric structures with atom numbering of 2,4-dmpba.

differences compared to $ct(C_s)$ and $ct(C_1)$ isomers are more than 2.0 kcal/mol. As for the $ct(C_s)$ and $ct(C_1)$, the following equations can be written for the mole fractions of individual conformers:



According to equilibrium given above, we can write

$$K_c = N_a/N_b \text{ and } N_a + N_b = 1$$

where K_c is conformational equilibrium constant between a and b forms, N_a and N_b are mole fractions of conformers a and b .

Here $N_a = 1/(1 + K_c)$, $N_b = K_c/(1 + K_c)$, $K_c = e^{-\delta\Delta G/RT}$, $R = 1.987 \times 10^{-3}$ kcal/mol K, $T = 298$ K and $\delta\Delta G = \Delta G_b - \Delta G_a$ [37].

Regarding the calculated free energies for the gas phase, mole fractions of $ct(C_s)$ and $ct(C_1)$ are almost the same. Relative percentage of $ct(C_s)$ conformer is only slightly bigger than $ct(C_1)$ conformer.

4.2. Vibrational studies of 2,4-dmpba

2,4-dmpba consists of 24 atoms, so it has 66 normal vibrational modes and it belongs to the point group C_s in its

lowest energy case calculated at 6-31++G(d,p) level of theory. According to the calculations, 13 normal vibrational modes of the title molecule are below 400 cm^{-1} . C_s and C_1 point groups are possible for 2,4-dmpba as given in Table 2. Since the cis-trans conformation with C_s point group is the most stable one, all the experimental infrared and Raman results were compared to the theoretical results of $ct(C_s)$ form of 2,4-dmpba. The calculated infrared and Raman wavenumbers together with experimental data of the title molecule are presented in Table 3. Theoretical and experimental (IR and Raman) spectra of 2,4-dmpba are given in Figs. 2 and 3.

Calculated infrared intensities were modified by assigning the highest intensity peak to 100%. Calculated Raman activities were converted to relative Raman intensities (I_R) using the following relationship derived from the intensity theory of Raman scattering [38,39]:

$$I_i = \frac{f(\nu_0 - \nu_i)^4 S_i}{\nu_i [1 - \exp(-h\nu_i/kT)]}$$

where ν_0 is the laser exciting wavenumber in cm^{-1} (in this work, $\nu_0 = 18797 \text{ cm}^{-1}$), ν_i the vibrational wavenumber of the i^{th} normal mode and S_i is the Raman scattering activity of the normal mode ν_i , f (is a constant and in the present study, it is 10^{-14}) is a suitably chosen common normaliza-

Table 1
Optimized geometric parameters of 2,4-dmpba for ten conformers calculated by B3LYP with 6-31++G(d,p) basis set.

Parameters	B3LYP/6-311G(d,p)						Exp. [34]
	tt(C ₁)	ct(C ₁)	cc(C ₁)	tt(C _s)	ct(C _s)	cc(C _s)	
R(10;11)	0.964	0.969	0.968	0.964	0.969	0.968	
R(12;13)	0.963	0.966	0.961	0.963	0.966	0.961	
R(9;10)	1.375	1.371	1.363	1.375	1.371	1.363	1.362
R(9;12)	1.386	1.375	1.375	1.386	1.375	1.375	1.378
R(3;9)	1.561	1.567	1.584	1.561	1.567	1.584	1.568
R(3;4)	1.422	1.417	1.421	1.422	1.417	1.421	1.404
R(4;5)	1.397	1.392	1.393	1.397	1.392	1.393	1.378
R(5;1)	1.402	1.404	1.403	1.402	1.404	1.403	
R(1;2)	1.398	1.398	1.397	1.398	1.398	1.398	
R(2;23)	1.397	1.398	1.398	1.397	1.398	1.398	1.378
R(3;23)	1.404	1.402	1.402	1.404	1.402	1.401	1.404
R(4;8)	1.361	1.379	1.376	1.361	1.379	1.376	
R(8;14)	1.420	1.425	1.426	1.420	1.425	1.426	
R(1;18)	1.366	1.365	1.363	1.366	1.365	1.363	
R(18;19)	1.423	1.424	1.424	1.423	1.424	1.424	
R(14;17)	1.091	1.091	1.090	1.091	1.091	1.090	
R(19;20)	1.091	1.091	1.090	1.091	1.091	1.090	
R(5;7)	1.082	1.082	1.082	1.082	1.082	1.082	1.000
R(2;6)	1.083	1.083	1.083	1.083	1.083	1.083	1.000
R(23;24)	1.085	1.086	1.088	1.085	1.086	1.088	
A(9;10;11)	115.16	110.71	110.78	115.17	110.61	110.69	111.0
A(9;12;13)	115.97	111.54	115.10	115.99	111.54	115.08	111.0
A(10;9;12)	121.85	117.92	114.73	121.84	117.94	114.76	
A(4;3;9)	125.47	124.02	123.52	125.49	124.00	123.52	122.0
A(4;8;14)	119.31	119.41	119.70	119.33	119.42	119.73	
A(4;3;23)	116.31	116.24	115.29	116.32	116.25	115.31	120.0
A(8;14;17)	105.60	105.85	105.74	105.60	105.84	105.73	
A(4;5;1)	120.15	119.53	119.83	120.13	119.50	119.80	
A(5;1;2)	120.37	120.39	120.11	120.38	120.40	120.12	
A(1;5;7)	117.64	117.77	117.69	117.66	117.81	117.72	
A(1;18;19)	118.55	118.57	118.59	118.51	118.53	118.56	
A(18;19;20)	105.77	105.73	105.72	105.77	105.74	105.73	
A(1;2;6)	121.79	121.59	121.74	121.80	121.59	121.75	
A(2;23;24)	118.43	118.80	116.51	118.43	118.80	116.53	
A(15;14;16)	109.36	109.74	109.84	109.36	109.75	109.84	
A(21;19;22)	109.46	109.53	109.60	109.46	109.52	109.59	
D(11;10;9;3)	179.98	-0.01	-0.01	180.00	0.00	0.00	
D(10;9;3;4)	-0.14	0.01	0.00	0.00	0.00	0.00	
D(3;4;8;14)	-179.95	-179.99	179.99	180.00	180.00	180.00	
D(4;8;14;17)	179.94	179.99	-179.99	180.00	180.00	180.00	
D(8;4;5;7)	0.01	0.00	0.00	0.00	0.00	0.00	
D(4;5;1;18)	-180.00	180.00	179.99	180.00	180.00	180.00	
D(5;1;18;19)	179.99	180.00	179.99	180.00	180.00	180.00	
D(1;18;19;22)	61.25	61.25	61.29	61.23	61.23	61.26	
D(4;8;14;16)	61.23	61.22	61.28	61.30	61.25	61.29	
D(11;10;9;12)	-0.04	-180.00	179.99	0.00	180.00	180.00	

tion factor for all peak intensities. *h*, *k*, *c* and *T* are Planck and Boltzmann constants, speed of light and temperature in Kelvin, respectively.

The carbon–carbon stretching modes of the phenyl group occur in the range of 1620 to 1320 cm⁻¹ [40]. In

this study, the carbon–carbon stretching vibrations of 2,4-dmpba have been observed at 1605 (R), 1603 (IR), 1574 (IR, R), 1508 (IR) and 1505 cm⁻¹ (R). The corresponding theoretical values of these vibrations are 1615, 1574 and 1503 cm⁻¹. CH₃ antisymmetric and symmetric

Table 2
Geometry, point groups, mode distribution, optimized energy and energy differences of 2,4-dmpba calculated by B3LYP with 6-31++G(d,p) basis set.

Geometry	Point group	Mode distribution	Optimized energy (Hartree)	Energy differences ^a (kcal/mol)
Trans–trans	C ₁	66A	-637.209369	7.750
Cis–trans	C ₁		-637.221650	0.004
Cis–cis	C ₁		-637.215722	3.763
Trans–trans	C _s	43A'+23A''	-637.210064	7.314
Cis–trans	C _s		-637.221719	0.000
Cis–cis	C _s		-637.215950	3.620

^a Relative energy differences were calculated compared to ct(C_s) conformer.

Table 3

Comparison of the experimental and the calculated vibrational wavenumbers (cm^{-1}) of 2,4-dmpba.

M.	TED ($\geq 10\%$) ^a	Exp ^b		S. wavenumber		B3LYP/6-311+G(d,p)		
		IR	R	ν^α	ν^β	Cis–trans–Cs		
						ν^θ	I_{IR}	I_{R}
ν_{66}	$\nu\text{OH}(100)$	3480	–	3676	3445	3849	15.12	–
ν_{65}	$\nu\text{OH}(100)$	3339	–	3600	3374	3770	35.82	–
ν_{63}	$\nu_6-2(92)$	3063	3088	3084	3076	3229	1.80	44.29
ν_{61}	$\nu_{17-14}(84)$	3007	3010	3012	2998	3154	2.91	48.93
ν_{60}	$\nu_{20-19}(86)$	2996	2999	3012	2998	3154	5.01	51.33
ν_{59}	$\nu_{15-14}(50) + \nu_{16-14}(50)$	2972	2973	2959	2946	3098	6.10	23.94
ν_{58}	$\nu_{21-19}(50) + \nu_{22-19}(50)$	2946	2950	2949	2936	3088	7.14	27.57
ν_{57}	$\nu_{15-14}(44) + \nu_{16-14}(44)$	–	2882	2893	2880	3029	–	72.23
ν_{56}	$\nu_{21-19}(45) + \nu_{22-19}(45)$	2837	2841	2887	2873	3023	12.36	76.08
ν_{55}	$\nu_5-4(22) + \nu_{23-22}(18) + \nu_{23-3}(11) + \nu_5-1(10)$	1603	1605	1615	1614	1653	74.57	100.00
ν_{54}	$\nu_2-1(29) + \nu_4-3(15) + \nu_5-1(12) + \nu_{23-3}(11)$	1574	1574	1574	1575	1611	23.16	12.87
ν_{53}	$\nu_4-3(11) + \nu_5-1(11)$	1508	1505	1503	1501	1538	5.45	13.35
ν_{51}	$\delta_{21-19-22}(28)$	1463	–	1473	1466	1508	13.33	–
ν_{50}	$\delta_{15-14-16}(11)$	–	1450	1463	1454	1497	–	19.78
ν_{47}	$\delta_{20-19-18}(16) + \delta_{20-19-21}(14)$ $\delta_{20-19-22}(14) + \delta_{21-19-22}(14)$ $\delta_{21-19-18}(13) + \delta_{22-19-18}(13)$	–	1435	1443	1436	1477	–	8.38
ν_{46}^c	$\nu_{23-2}(8) + \delta_{15-14-17}(8)$ $\delta_{16-14-17}(8) + \nu_5-4(8)$	1417	1412	1421	1420	1455	28.42	1.28
ν_{45}	$\nu_{12-9}(39) + \nu_{10-9}(10) + \delta_{11-10-9}(10)$	1400	1391	1370	1375	1402	39.20	6.09
ν_{44}	$\nu_{10-9}(31) + \nu_9-3(19) + \delta_{13-12-9}(10)$	1342	1325	1345	1350	1377	100.00	42.04
ν_{43}	$\nu_{23-3}(19) + \nu_2-1(15) + \nu_4-3(14)$	1298	1299	1308	1306	1339	32.70	25.59
ν_{42}	$\nu_{18-1}(20) + \nu_{23-2}(10)$	1280	–	1280	1277	1310	27.44	–
ν_{41}	$\delta_{24-23-3}(21) + \nu_{23-3}(14)$ $\delta_{24-23-2}(11) + \nu_8-4(10)$	1256	1262	1255	1253	1285	21.51	23.85
ν_{40}	$\delta_{17-14-8}(18) + \nu_8-4(14)$	1207	1207	1208	1202	1236	33.64	5.39
ν_{39}	$\delta_{20-19-18}(29) + \delta_{17-14-8}(17)$	1185	1186	1180	1175	1208	0.45	9.70
ν_{38}	$\delta_{17-14-8}(13) + \delta_{20-19-18}(12) + \nu_8-4(11)$ $\delta_7-5-4(10)$	1153	1152	1158	1153	1185	32.55	3.19
ν_{37}	$\nu_{23-2}(25) + \delta_6-2-23(18) + \delta_6-2-1(12)$	1120	–	1145	1142	1172	18.32	–
ν_{34}	$\delta_{11-10-9}(26)$	1094	1110	1101	1101	1127	0.32	28.05
ν_{33}	$\delta_{11-10-9}(26) + \nu_{14-8}(21) + \nu_{12-9}(10)$	1051	1048	1059	1055	1084	20.01	8.82
ν_{31}	$\nu_{14-8}(19) + \delta_{11-10-9}(16) + \delta_{13-12-9}(15)$	1033	1016	1024	1027	1048	13.31	12.56
ν_{30}	$\delta_{13-12-9}(50) + \nu_{10-9}(25) + \nu_{12-9}(16)$	1013	992	985	982	1008	30.62	5.35
ν_{28}	$\nu_{19-18}(19) + \nu_8-4(16) + \nu_{18-1}(11)$	911	916	913	914	935	2.49	26.38
ν_{27}	$\tau_7-5-4-8(27) + \tau_7-5-1-18(26)$ $\tau_7-5-4-3(13) + \tau_7-5-1-2(10)$ 820	819	–	–	–	–	–	–
ν_{26}	$\tau_6-2-1-18(25) + \tau_3-23-2-6(22)$ $\tau_6-2-1-5(15)$	773	–	797	791	816	2.00	–
ν_{25}	$\nu_2-1(12) + \nu_4-3(11) + \delta_2-23-3(11)$	739	–	730	732	747	5.16	–
ν_{24}	$\tau_7-5-4-3(10) + \tau_{10-9-3-4}(10)$	–	734	726	726	743	–	60.62
ν_{23}	$\tau_{11-10-9-12}(53) + \tau_{11-10-9-3}(42)$	681	674	671	666	687	10.35	1.43
ν_{22}	$\nu_9-3(22) + \nu_{18-1}(10)$	658	659	660	665	676	1.12	7.41
ν_{21}	$\tau_{13-12-9-10}(15)$	640	–	646	643	661	10.42	–
ν_{20}	$\tau_{13-12-9-10}(11)$	614	–	620	617	635	6.65	–
ν_{19}	$\delta_{19-18-1}(14) + \delta_5-4-8(13) + \delta_2-1-18(11)$	603	607	595	606	609	0.81	12.28
ν_{18}	$\nu_8-4(14) + \delta_5-4-3(11)$	545	–	528	534	540	16.66	–
ν_{17}	$\tau_{13-12-9-3}(50) + \tau_{13-12-9-10}(28)$	533	535	527	524	539	0.57	29.44
ν_{15}	$\tau_3-23-2-1(15) + \tau_2-23-3-4(13)$ $\tau_{23-2-1-18}(10)$	455	457	452	449	463	3.46	2.97

ν^α and ν^β : scaled with 0.955 above 1800 cm^{-1} , 0.977 under 1800 cm^{-1} [43]; ν^s : wavenumbers are scaled by SQM methodology, ν^θ : unscaled wavenumbers; M: mode; IR: infrared; R: Raman; I_{IR} and I_{R} : infrared and Raman intensities; Exp.: experimental.

^a Our vibrational wavenumbers assignments on the basis of total energy distribution (TED) calculations.

^b Our experimental IR and Raman wavenumbers, ν , δ , τ : stretching, bending and torsion, respectively.

^c TED ≥ 8 .

vibrations arise between the region of $1508\text{--}1417\text{ cm}^{-1}$. O–B–O antisymmetric stretching vibrations were observed at 1391 (R) and 1362 cm^{-1} (IR). CH stretching vibrations for heteroaromatic structures are commonly appeared in the region of $3000\text{--}3200\text{ cm}^{-1}$. In the high wavenumber region, CH stretching modes of phenyl ring were observed at 3088 (R) and 3063 cm^{-1} (IR). In the OH region, very strong and broad-band in the spectra of some

boronic acid molecules occur at $\sim 3300\text{ cm}^{-1}$. In the spectra of phenylboronic acid, [41] and 4-pyridineboronic acids, [42], absorption bands were observed at 3280 and 3467 cm^{-1} , respectively. Special attention is required for OH vibrations of the title molecule. Four OH stretching modes are observed at $3480\text{--}3262\text{ cm}^{-1}$ in the FT-IR spectrum for 2,4-dmpba. Two of them are broad while the remaining two have comparatively lower line

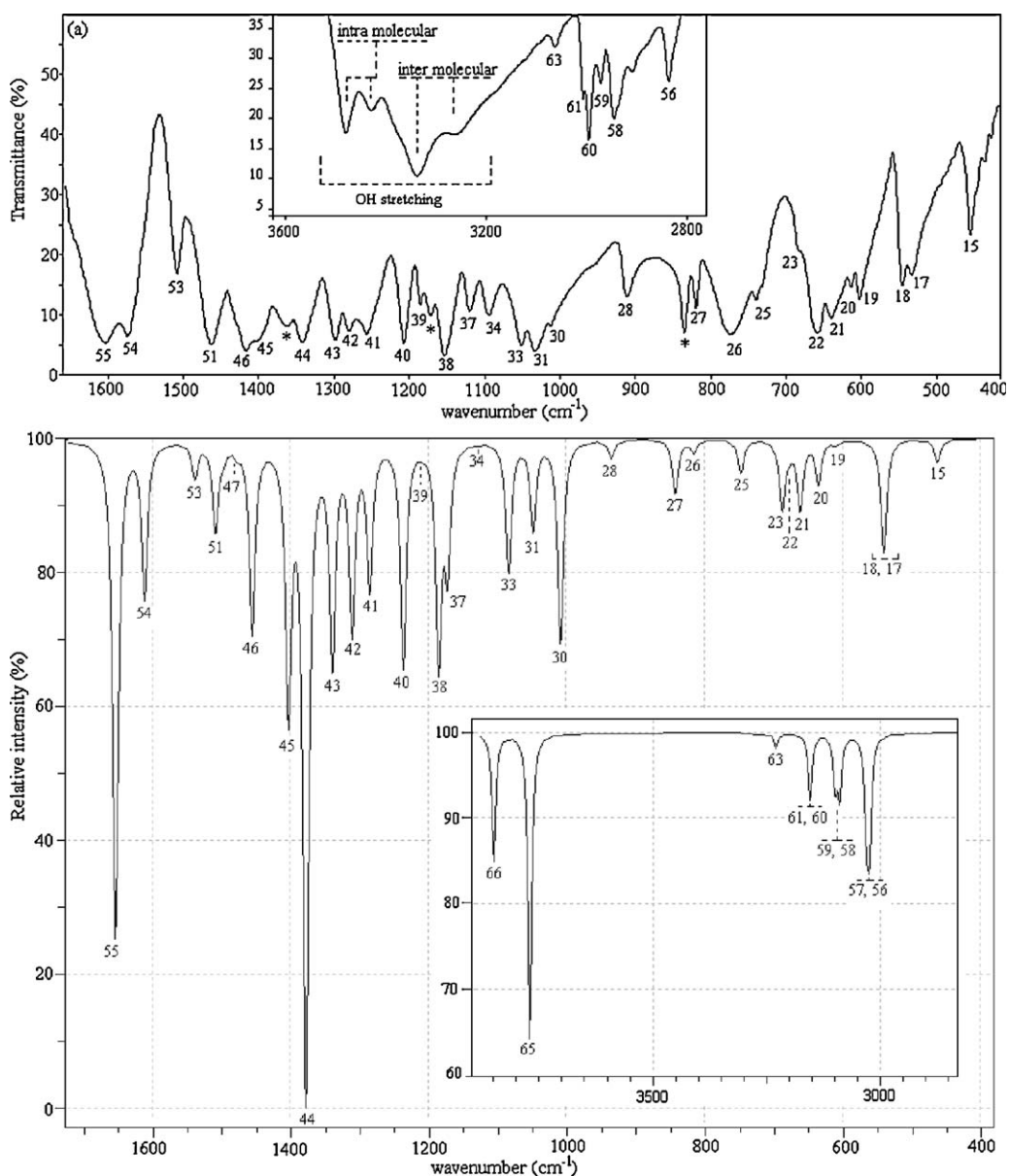


Fig. 2. Experimental (a) and unscaled calculated (b) infrared spectra of 2,4-dmpba (mode numbers are given above the respective peaks).

width. These results suggest that some of O(11)H possibly include in the formation of intramolecular hydrogen bonding, which lead to two OH bands at 3480 and 3431 cm^{-1} . Likewise, O(12)H tends to be involved in intermolecular hydrogen bonding, resulting in two broad OH bands at 3339 and 3262 cm^{-1} . In short, as seen in Fig. 3a, multiple OH bands could be attributed to potential inter–intra molecular interactions. We also made measurements in the frequency region of $1300\text{--}200\text{ cm}^{-1}$. These vibrations have revealed to be mixed type of vibrations as given in Table 3. In general, B3LYP/6-31++G(d,p) level of calculation with dual scaling factors used in this study [43] provided reasonable agreement with the experimental findings. The results obtained in this study also indicate that B3LYP/6-31++G(d,p) method

is reliable and it makes easier the understanding of vibrational spectrum and structural parameters of 2,4-dmpba. In general, B3LYP/6-31++G(d,p) level of calculation with the dual scaling factors [43] and SQM [17,29] methodology used in this study provided reasonable agreement with the experimental findings. The results obtained in this study also indicate that B3LYP/6-31++G(d,p) method is reliable and it makes easier the understanding of vibrational spectrum and structural parameters of 2,6-dmpba. However, during the approximate mode explanations, intra–intermolecular interactions should be taken notice as calculations were performed for a single molecule, which disregards intermolecular interactions. For instance, as in the case observed for OH vibrations, OH groups, which possess

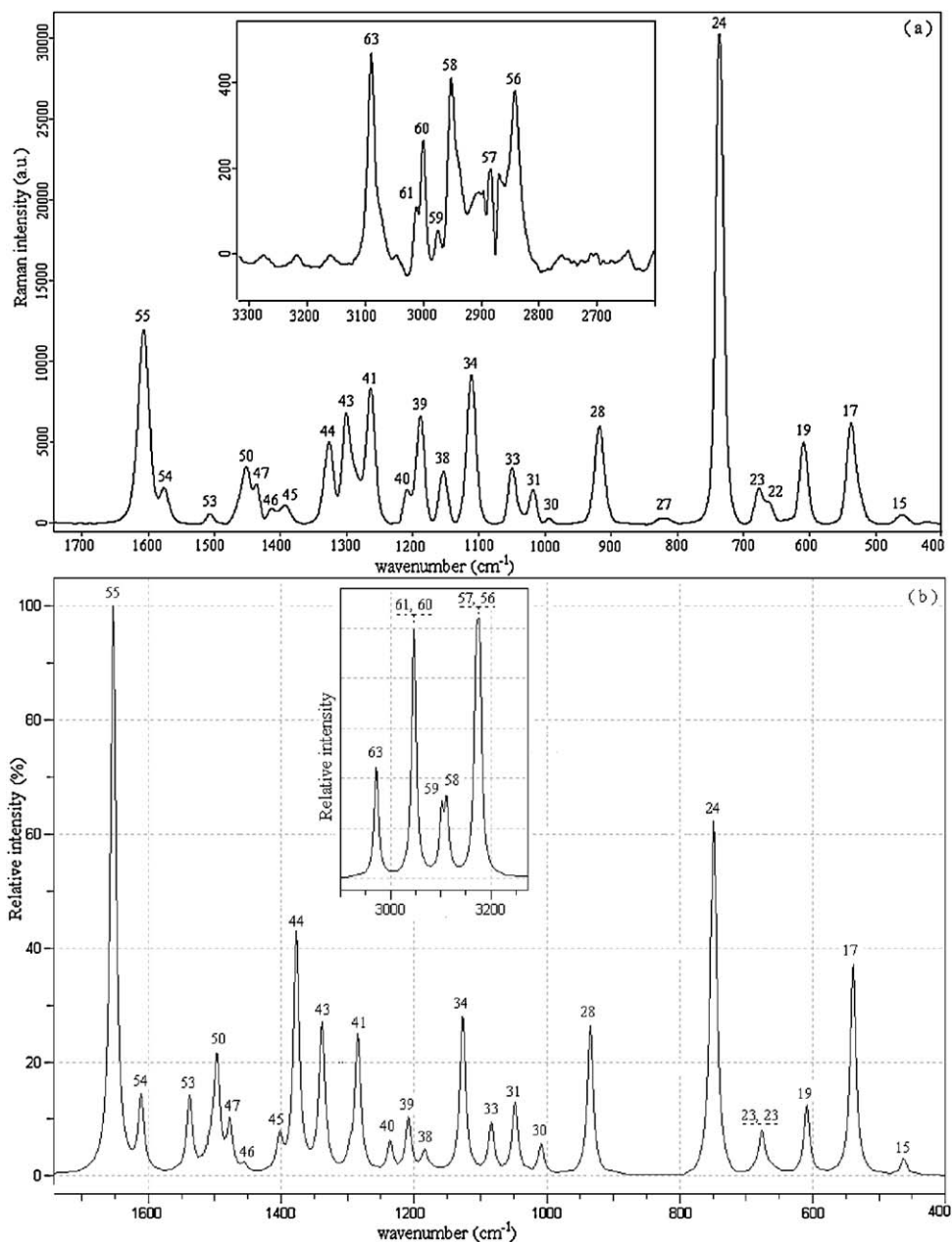


Fig. 3. Experimental (a) and unscaled calculated (b) Raman spectra of 2,4-dmpba (mode numbers are given above the respective peaks).

intramolecular hydrogen bonding, have lower line width and they appear in the high frequency region compared to broad OH vibrational bands indicating intermolecular hydrogen bonding. In the theoretical calculations, the latter was appeared in the high frequency region. The peaks marked with asterisks in Fig. 2 were possibly due to the hydrogen bonding interactions or they are not available with ct(Cs) conformer.

4.3. NMR studies of 2,4-dmpba

All the experimental and theoretical chemical shift values for ^{13}C (CP/MAS) NMR and ^1H measurements are

given in Table 4. Considering the chemical environment, 2,4-dmpba shows seven different carbon atoms in its solution state ^{13}C NMR spectrum (Fig. 4a), which is surprisingly not in agreement with the structure regarding molecular symmetry. C_2 and C_3 seem to have equal chemical shieldings, therefore, they give a singlet. Contrary to averaged solution ^{13}C NMR values, in ^{13}C /MAS NMR spectrum of 2,4-dmpba (Fig. 4b), C_3 gives another broad singlet, which indicates that the chemical environment of C_3 in the powder form is different than C_3 in the solution form or intramolecular rotation is inhibited. Broadening of C_3 is probably due to boron-11, which is a quadrupolar nucleus of spin 1 and so its

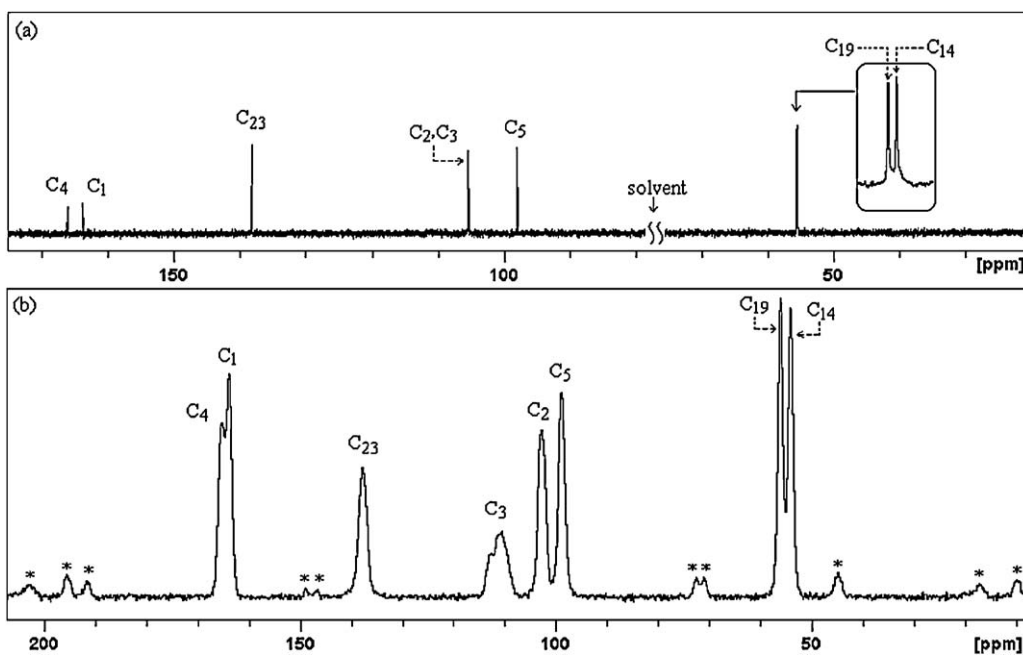


Fig. 4. ¹³C NMR (a) and ¹³C (CP/MAS) NMR (b) spectra of 2,4-dmpba (* indicates spinning sidebands).

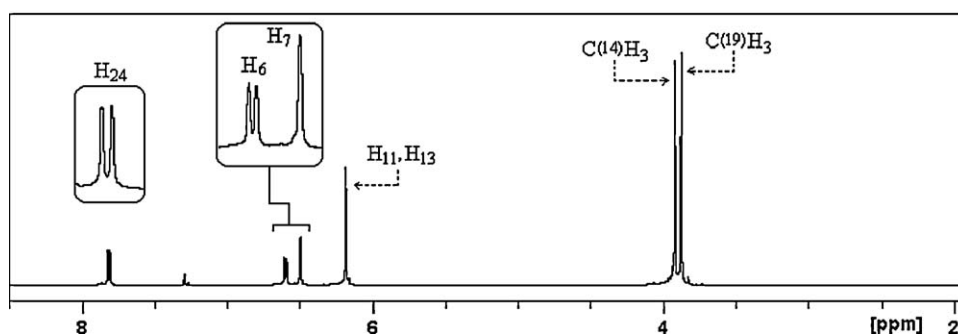


Fig. 5. ¹H NMR spectrum of 2,4-dmpba.

Table 4
Experimental and calculated ¹³C and ¹H NMR chemical shifts (ppm) of 2,4-dmpba.

Nucleus	Experimental (ppm)	Calculated (ppm)	
	Liquid/solid phase	ct (C ₁)	ct (C _s)
C ₄	166.45/165.23	163.37	164.58
C ₁	164.05/163.81	160.47	161.04
C ₂₃	138.37/137.71	137.01	136.87
C ₃	105.49/112.96–108.69 ^a	109.04	107.69
C ₂ , C ₃	105.49/102.70	103.62	103.03
C ₅	98.29/98.79	95.56	96.04
C ₁₉	56.62/56.30	55.01	55.33
C ₁₄	55.51/54.12	54.69	54.67
H ₂₄	7.81	8.26	8.18
H ₆	6.59	6.68	6.75
H ₇	6.49	6.52	6.57
H ₁₁	6.18	7.06	7.20
H ₁₃	6.18	5.05	5.06
C(14)H ₃	3.92	3.94	3.95
C(19)H ₃	3.87	3.89	3.95

^a Cannot be cited with high accuracy.

anisotropy is strongly dependent on *x*, *y* and *z* coordinates relative to boron-11 located at the origin or (0,0). Solution to solid chemical shifts ($\Delta = \delta_{\text{solution}} - \Delta = \delta_{\text{solid}}$) reflect intermolecular and intramolecular interactions [18]. The biggest chemical shift differences for carbon between the solid and solution states are 2.79 ppm (C₃), which confirm the presence of inter-intramolecular hydrogen bondings, where H₁₁ and H₁₃ are possibly involved. According to the obtained ¹H NMR spectrum of the title compound (Fig. 5), protons of OH appear as a singlet at 6.18 ppm, which indicates that both OH protons have the similar chemical environment in solution state, which also requires hydrogen bonding. H₆ appears as doublet at 6.59 ppm due to only one neighboring proton. H₇ group gives a singlet at 6.49 ppm. Methoxy protons appear at 3.92 and 3.87 ppm. The correlations between C₁₄–H_{15–17}, C₁₉–H_{20–22}, C₅–H₇, C₂–H₆ and C₂₃–H₂₄ are clearly observed in HETCOR spectrum (Fig. 6).

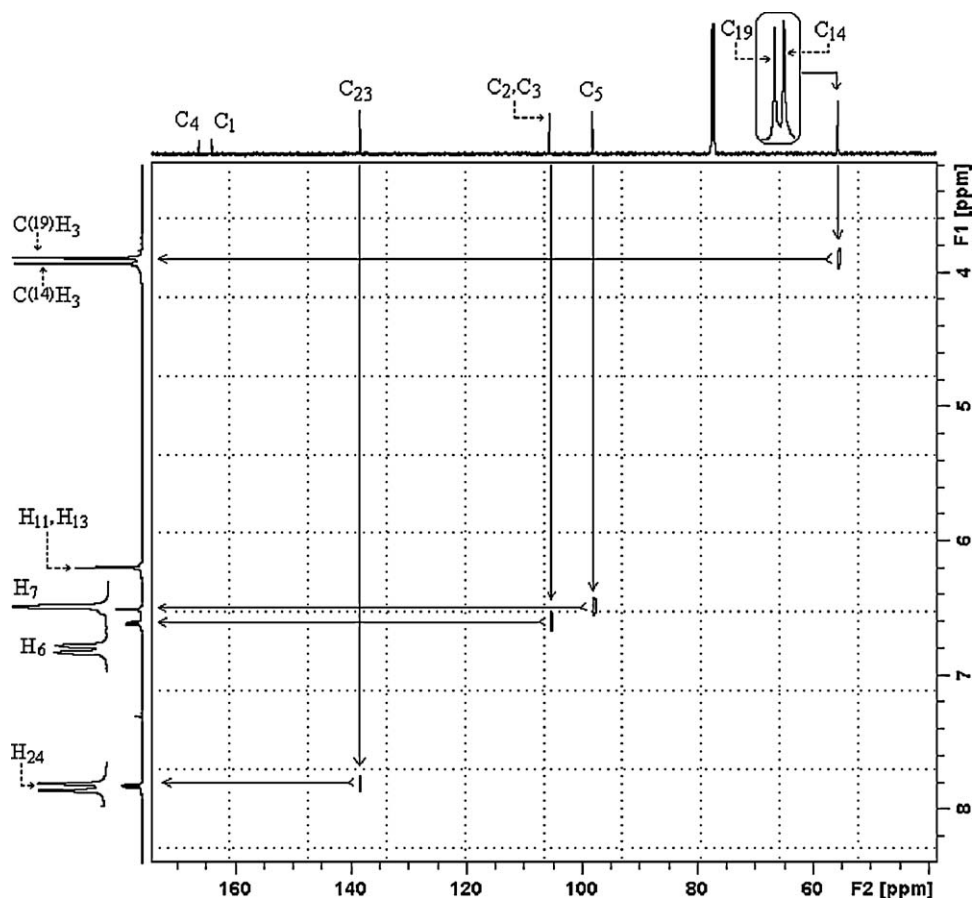


Fig. 6. HETCOR NMR spectrum of 2,4-dmpba.

5. Conclusion

This article presents the experimental and theoretical vibrational IR, Raman and (CP/MAS) NMR spectra of 2,4-dmpba molecules. The FT-IR and FT-Raman spectra have been recorded in the range 4000–400 cm^{-1} . Due to the lack of experimental information on the structural parameters available in the literature, theoretical calculations were compared with those for a similar molecule. Some important vibrational bands have been discussed and assigned based on the calculated infrared and Raman intensities. The molecular geometry and all of the vibrational wavenumbers and nuclear magnetic shieldings of 2,4-dmpba in the ground state have been calculated using the density functional method B3LYP/6-31++G(d,p) level. Based on the theoretical calculations following six different molecular structures were proposed: tt(C₁), ct(C₁), cc(C₁), tt(Cs), ct(Cs) and cc(Cs). Optimized energies of the proposed structures indicate that ct(Cs) and ct(C₁) are the most stable conformers. Any differences observed between the experimental and the calculated wavenumbers and chemical shifts could be due to the fact that the calculations have been performed for single molecule in the gaseous state contrary to the experimental values recorded in the presence of intermolecular interactions, which is the case in present study and revealed by ¹³C CP/

MAS NMR measurements. Henceforth, the assignments made at B3LYP/6-31++G(d,p) level of theory with only reasonable deviations from the experimental values seem feasible.

References

- [1] W. Tjarks, A.K.M. Anisuzzaman, L. Liu, S.H. Soloway, R.F. Barth, D.J. Perkins, D.M. Adams, *J. Med. Chem.* 35 (1992) 16228.
- [2] Y. Yamamoto, *Pure Appl. Chem.* 63 (1991) 423.
- [3] F. Alam, A.H. Soloway, R.F. Barth, N. Mafune, D.M. Adam, W.H. Knoth, *J. Med. Chem.* 32 (1989) 2326.
- [4] M.R. Stabile, et al. *Bioorg. Med. Chem. Lett.* 21 (1996) 2501.
- [5] P.R. Westmark, B.D. Smith, *J. Pharm. Sci.* 85 (1996) 266.
- [6] N.A. Petasis, *Aust. J. Chem.* 60 (2007) 795.
- [7] E. Cuthbertson, *Boronic Acids: Properties and Applications*, Alfa Aesar, Heysham, 2006.
- [8] D.G. Hall (Ed.), *Boronic Acids: Preparation, Applications in Organic Synthesis and Medicine*, Wiley-VCH, Weinheim, 2005.
- [9] A.H. Soloway, R.G. Fairchild, *Sci. Am.* 262 (1990) 100.
- [10] X. Chen, G. Liang, D. Whitmire, J.P. Bowen, *J. Phys. Org. Chem.* 11 (1988) 378.
- [11] N.C. Handy, P.E. Maslen, R.D. Amos, J.S. Andrews, C.W. Murray, G.J. Laming, *Chem. Phys. Lett.* 197 (1992) 506.
- [12] N.C. Handy, C.W. Murray, R.D. Amos, *J. Phys. Chem.* 97 (1993) 4392.
- [13] P.J. Stephens, F.J. Devlin, C.F. Chabalowski, M.J. Frisch, *J. Phys. Chem.* 98 (1994) 11623.
- [14] F.J. Devlin, J.W. Finley, P.J. Stephens, M.J. Frisch, *J. Phys. Chem.* 99 (1995) 16883.
- [15] S.Y. Lee, B.H. Boo, *Bull. Korean Chem. Soc.* 17 (1996) 754.
- [16] S.Y. Lee, B.H. Boo, *Bull. Korean Chem. Soc.* 17 (1996) 760.
- [17] G. Rauhut, P. Pulay, *J. Phys. Chem.* 99 (1995) 3093.

- [18] T. Żołek, K. Paradowska, I. Wawer, *Solid State Nucl. Magn. Reson.* 23 (2003) 77.
- [19] M. Şenyel, A. Ünal, Ö. Alver, *C. R. Chimie* 12 (2009) 808.
- [20] Z. Meng, W.R. Carper, *J. Mol. Struct. Theochem* 588 (2002) 45.
- [21] K. Paradowska, M. Wolniak, M. Pisklak, J.A. Gliński, M.H. Davey, I. Wawer, *Solid State Nucl. Magn. Reson.* 34 (2008) 202.
- [22] L. Depature, G. Surpateanu, *Spectrochim. Acta A* 59 (2003) 3029.
- [23] Z. Dega-Szafran, A. Katrusiak, M. Szafran, *J. Mol. Struct.* 785 (2006) 160.
- [24] H. Dodziuk, O.M. Demchuk, W. Schilf, G. Dolgonos, *J. Mol. Struct.* 693 (2004) 145.
- [25] H. Beraldo, W.F. Nacif, D.X. West, *Spectrochim. Acta A* 57 (2001) 1847.
- [26] A.A. Abdel-Shafi, *Spectrochim. Acta A* 57 (2001) 1819.
- [27] A.C. de Dios, C.J. Jameson, *Ann. Rep. NMR Spectrosc.* 29 (1994) 1.
- [28] A.C. de Dios, *Prog. Nucl. Magn. Reson. Spectrosc.* 29 (1996) 229.
- [29] J. Baker, A.A. Jarzecki, P. Pulay, *J. Phys. Chem. A* 102 (1998) 1412.
- [30] S. Miertus, E. Scrocco, J. Tomasi, *Chem. Phys.* 55 (1981) 117.
- [31] K. Wolinski, J.F. Hinton, P. Pulay, *J. Am. Chem. Soc.* 112 (1990) 8251.
- [32] M.J. Frisch, G.W. Trucks, H.B. Schlegel, G.E. Scuseria, M.A. Robb, J.R. Cheeseman, J.A. Montgomery, J.T. Vreven, K.N. Kudin, J.C. Burant, J.M. Millam, S.S. Iyengar, J. Tomasi, V. Barone, B. Mennucci, M. Cossi, G. Scalmani, N. Rega, G.A. Petersson, H. Nakatsuji, M. Hada, M. Ehara, K. Toyota, R. Fukuda, J. Hasegawa, M. Ishida, T. Nakajima, Y. Honda, O. Kitao, H. Nakai, M. Klene, X. Li, J.E. Knox, H.P. Hratchian, J.B. Cross, C. Adamo, J. Jaramillo, R. Gomperts, R.E. Stratmann, O. Yazyev, A.J. Austin, R. Cammi, C. Pomelli, J.W. Ochterski, P.Y. Ayala, K. Morokuma, G.A. Voth, P. Salvador, J.J. Dannenberg, V.G. Zakrzewski, S. Dapprich, A.D. Daniels, M.C. Strain, O. Farkas, D.K. Malick, A.D. Rabuck, K. Raghavachari, J.B. Foresman, J.V. Ortiz, Q. Cui, A.G. Baboul, S. Clifford, J. Cioslowski, B.B. Stefanov, G. Liu, A. Liashenko, P. Piskorz, I. Komaromi, R.L. Martin, D.J. Fox, T. Keith, M.A. Al-Laham, C.Y. Peng, A. Nanayakkara, M. Challacombe, P.M.W. Gill, B. Johnson, W. Chen, M.W. Wong, C. Gonzalez, J.A. Pople, Gaussian 03 Revision C.02 Gaussian Inc, Pittsburgh PA, 2003.
- [33] M.K. Cyrański, A. Jezińska, P. Klimentowska, J.J. Panek, A. Sporzyński, *J. Phys. Org. Chem.* 21 (2008) 472.
- [34] P.N. Horton, M.B. Hursthouse, M.A. Becket, M.P.R. Hankey, *Acta Cryst. E Struct. Rep.* E60 (2004) o2204.
- [35] K.L. Bhat, N.J. Howard, H. Rostami, J.H. Lai, C.W. Bock, *J. Mol. Struct. (Theochem)* 723 (2005) 147.
- [36] S.J. Rettig, J. Trotter, *Can. J. Chem.* 55 (1977) 3071.
- [37] D. Hür, A. Güven, *J. Mol. Struct. (Theochem)* 583 (2002) 1.
- [38] G. Keresztury, S. Holly, J. Varga, G. Besenyi, A.Y. Wang, J.R. Durig, *Spectrochim. Acta A* 49A (1993) 2007.
- [39] G. Keresztury, *Raman spectroscopy; theory*, in: J.M. Chalmers, P.R. Griffiths (Eds.), *Handbook of Vibrational Spectroscopy*, vol.1, Wiley, 2002.
- [40] J.A. Faniran, H.F. Shurvell, *Can. J. Chem.* 46 (1968) 2089.
- [41] S.H. Brewer, A.M. Allen, S.E. Lappi, T.L. Chase, K.A. Briggman, C.B. Gorman, S. Franzen, *Langmuir* 20 (2004) 5512.
- [42] M. Kurt, T.R.M. Sertbakan, Özduran, *Spectrochim. Acta, Part A* 70 (2008) 664.
- [43] K. Balcı, S. Akyüz, *Vib. Spectrosc.* 48 (2008) 215.